ELSEVIER

PII: S0266-3538(97)00237-6

Composites Science and Technology 58 (1998) 1667–1673

Printed in Great Britain
0266-3538/98 $—see front matter

EXPERIMENTAL INVESTIGATION OF THE SHEAR STRENGTH OF A UNIDIRECTIONAL CARBON/ALUMINUM COMPOSITE UNDER DYNAMIC TORSIONAL LOADING

L. H. Dai,[a]* Y. L. Bai[a] & S.-W. R. Lee[b]

[a]*LNM, Institute of Mechanics, Chinese Academy of Sciences, Beijing 100080, People's Republic of China*
[b]*Department of Mechanical Engineering, Hong Kong University of Science & Technology, Kowloon, Hong Kong*

(Received 10 January 1997; revised 24 October 1997; accepted 11 December 1997)

Abstract

In this paper, the dynamic shear strength of a unidirectional C/A356·0 composite and A356·0 alloy, respectively, are measured with a split Hopkinson torsional bar (SHTB) technique. The results indicate that the carbon fibers make very little contribution to the enhancement of the shear strength of the matrix material. The microscopic inspections on the fracture surface of the composite show a multi-scale zigzag feature. This implies that there is a complicated shear failure mechanism in the unidirectional carbon/aluminum composite. © *1998 Elsevier Science Ltd. All rights reserved*

Keywords: A. metal-matrix composites, B. fracture, split Hopkinson torsion bar (SHTB), high strain rate, shear strength

1 INTRODUCTION

Shear strength and failure mechanism are two of the most significant problems for fiber-reinforced composites. With increasing applications and development of fiber-reinforced metal-matrix composites (MMCs) in aerospace, high-speed trains, and automotive industries, the understanding of shear behaviours of MMCs becomes more and more important.

In the past decade, there have been several attempts to study the dynamic shear response and fracture behaviour of fiber-reinforced polymer-matrix composites (FRPs) by split Hopkinson bar technique with a variety of shear loadings and specimen geometries. Among them, the use of the split Hopkinson torsional bar (SHTB) for the study of the dynamic shear behaviours of FRPs seems to be the most effective approach. The first two attempts to use SHTB were made by Parry and Harding[1] and Chiem and Liu,[2] in which the short thin-walled and cuboid specimens were adopted, respectively. A very significant increase in shear strength with respect to strain rates was observed for both woven and cross-ply glass/epoxy composite specimens. More recently, the SHTB was also used by Leber and Lifshitz[3] to investigate the shear response of plain-weave fiber-reinforced laminates, in which thin-walled tubular specimens with a large aspect ratio were used. Their results showed that the material exhibits high sensitivity to loading rates.

There were other efforts to use the split Hopkinson pressure bar (SHPB) for the study of the shear strength of FRPs. In 1986, Werner and Dharan[4] performed a test based upon the short-beam shear of SHPB to investigate the interlaminar and the transverse shear strength of plain-weave carbon/epoxy laminates. Their results showed no significant effect from strain rate. Bouette *et al.*[5] used a double-notched specimen of unidirectional carbon/epoxy composite. They also conducted a finite-element stress analysis and found large shear stress concentrations at the notch area. In addition, Harding *et al.*[6,7] suggested a double-lap and a single-lap shear specimen consecutively to determine the interlaminar shear strength of composite laminates.

Although great progress has been made in the investigation of the dynamic shear strength of FRPs at high strain rates, very little attention has been paid to that of MMCs. The present work is an attempt to characterize the dynamic shear strength of unidirectional carbon/aluminum composite. The experiments were conducted for both a unidirectional carbon-fiber reinforced A356·0 aluminum-matrix composite (C/A356·0) and A356·0 aluminum alloy with a modified split Hopkinson torsional bar. The dynamic shear strengths of the two materials were obtained and compared. The fracture surfaces of the C/A356·0 composite specimens were inspected with a scanning electronic microscope (SEM) and an interesting multi-scale zigzag feature was identified.

*To whom correspondence should be addressed at: Department of Mechanics, Peking University, Beijing 100871, People's Republic of China.

2 EXPERIMENTAL INVESTIGATION

2.1 Specimen preparation

The unidirectional C/A356·0 composite and A356·0 aluminum alloy were fabricated by pressure-infiltration casting (PIC) under the same conditions. This method allows inexpensive development and production of composite materials, and has found wide applications. In the literature, there are three different configurations for the PIC process, namely, top-filled, top-poured, and bottom-filled casting. In the present study, the last configuration was adopted. The schematic diagram for this fabrication process is shown in Fig. 1. In brief, a block of A356·0 aluminum was placed in a crucible which resides in a melting furnace inside a pressure chamber. A bundle of unidirectional carbon fiber pre-form was inserted into a quartz tube which is above the crucible. The crucible was heated in vacuum to prevent the metal from oxidation. Once the aluminum block was melted, the crucible was lifted up to immerse the carbon-fiber pre-form. Then the chamber was pressurized to enhance the infiltration of liquid metal into the carbon fibers. At last, the furnace was cooled down to a designated temperature and an MMC rod by PIC was formed. In this study, the cast specimen was a cylindrical bar with diameter of 22 mm. The carbon fibers were aligned along the longitudinal direction of the bar. The fiber volume fraction was 50%. For the fabrication of A356·0 aluminum alloy specimens, all procedures remained the same as above except that there was no fiber pre-form. The microstructure of the unidirectional C/A356·0 composite is shown in Fig. 2. The nominal properties of the fiber and matrix alloy are listed in Table 1.

Both C/A356·0 composite and A356·0 aluminum alloy in the present investigation were short thin-walled tubular specimens. The gauge length and thickness of specimen ranged within 1·9–2·1 mm and 0·5–0·7 mm, respectively. The fibers were aligned with the direction of the torsional axis. The characteristic dimensions of specimen are given in Fig. 3.

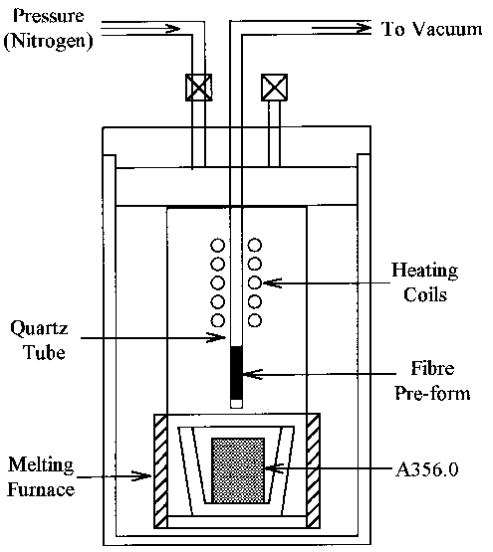

Fig. 1. Schematic diagram for pressure-infiltration casting.

2.2 Testing procedures

A schematic diagram of the split Hopkinson torsional bar (SHTB) used in the present study is shown in Fig. 4. Since the SHTB has many advantages over other apparatus, it is widely used to characterize the shear behaviour of materials subjected to high strain rates.[8]

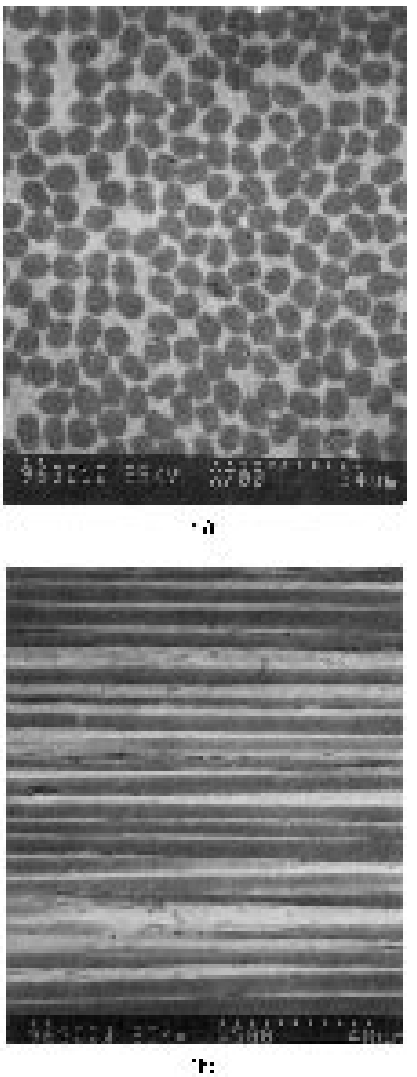

Fig. 2. SEM Micrographs of C/A356·0 composite: (a) cross-section view from the fiber direction; (b) cross-section view from the transverse direction.

Table 1. Nominal properties of fiber and matrix of the C/A356·0 composite

	Fiber	Matrix
Type	T-300	A356·0 Al (7·0Si–0·35 Mg–0·1Ti)
Diameter	7 μm	
Tensile strength	3500 MPa	182 MPa
Tensile modulus	235 GPa	80 GPa
Density	1·76 g cm^{-3}	2·72 g cm^{-2}

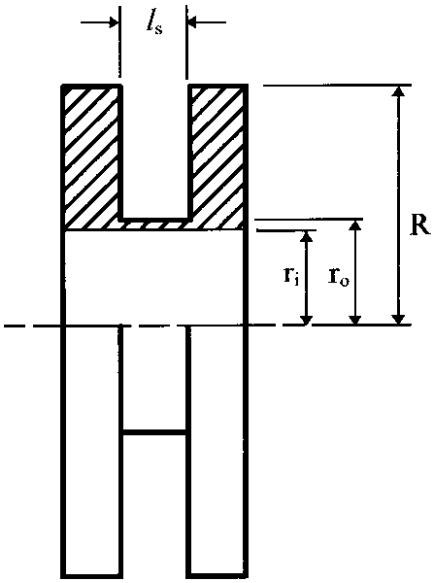

Fig. 3. Dimensions of the thin-walled tubular specimen ($l_s = 2$mm, $r_o = 5{\cdot}6$mm, $r_i = 5$mm, $R = 10$mm).

In the experiment, the short thin-walled tubular specimen was sandwiched between the input and output bars which have a diameter of 25 mm. At first, a hydraulic pump was actuated to twist the front portion of the input bar in order to store torsional energy between the rotating head and the clamp. The twisting torque was monitored by a static shear strain gauge as shown in Fig. 4. As the clamp was abruptly released, a torsional impulse propagated through the input bar and loaded the specimen. At the interface, part of the torsional wave reflected back to the input bar and the remaining energy was transmitted into the output bar via the specimen. According to the elastic properties of the bars and the recorded wave forms, the dynamic shear stress-strain in the specimen can be determined.

The incident, reflected, and transmitted pulses were measured by two sets of 90° rosette strain gauges mounted on the input and output bars, respectively. The signals from the input and output bars were conditioned by dynamic strain amplifiers and a Nicolet-4094 digital oscilloscope was used for data acquisition. Therefore, the shear stress, shear strain rate, and shear strain can be calculated according to the wave forms of the incident torque, M_i, and the reflected torque, M_r measured by the gauges on the input bar and the transmitted torque, M_t measured by the gauges on the output bar as follows:[8]

$$\tau = \frac{M_t(t)}{2\pi r_s^2 \delta} \tag{1}$$

$$\dot{\gamma} = \frac{2r_s C_0}{l_s J_b G_b}(M_i(t) - M_t(t)) \tag{2}$$

$$\gamma = \frac{2r_s C_0}{l_s J_b G_b}\int_0^t (M_i(t) - M_t(t))dt \tag{3}$$

Where l_s, r_s, δ are the gauge length, mean radius, and thickness of the specimen, respectively. In addition, C_0, J_b, G_b are the elastic wave speed, the polar moment of inertia, and shear modulus of the bars, respectively.

3 RESULTS AND DISCUSSION

A series of torsional impact tests ($\dot{\gamma} = 10^2 \sim 10^3$ 1/s) were conducted with the SHTB for both unidirectional C/A356·0 composite and A356·0 aluminum alloy. Figures 5 and 6 present typical oscilloscope signals from the tests on the composite and the matrix alloy, respectively. In each figure, the top trace gives the incident and reflected strain pulses while the bottom trace gives the transmitted strain pulse. The dynamic shear strength is defined as the shear stress corresponding to the peak point in the transmitted wave. This value can be obtained from eqn (1) with maximum M_t from

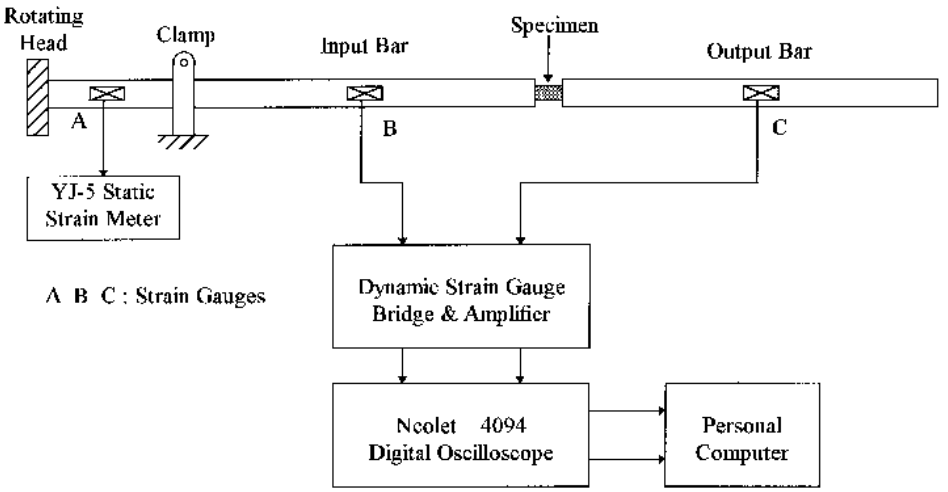

Fig. 4. Schematic diagram for the split hopkinson torsional bar testing system.

measurement. The average dynamic shear strength for the composite and the matrix, respectively, are given in Table 2. The typical shear stress/strain relation for both kinds of specimens are shown in Figs 7 and 8. The results show that the dynamic shear strength of the unidirectional C/A356·0 composite is almost the same as that of the matrix alloy. This indicates that the current carbon-fiber orientation which aligns with the torsional loading axis does not improve the shear strength of the matrix material effectively.

Table 2. Dynamic shear strength

Material	Shear strength (MPa)	Quantity of specimen
A356·0	321 ±3	5
C/A356·0	329 ±7	5

From the shear stress/strain relationship shown in Figs 7 and 8, one can find that the shear response of the matrix is quite different from that of the composite. The composite shows a rather more brittle failure than the

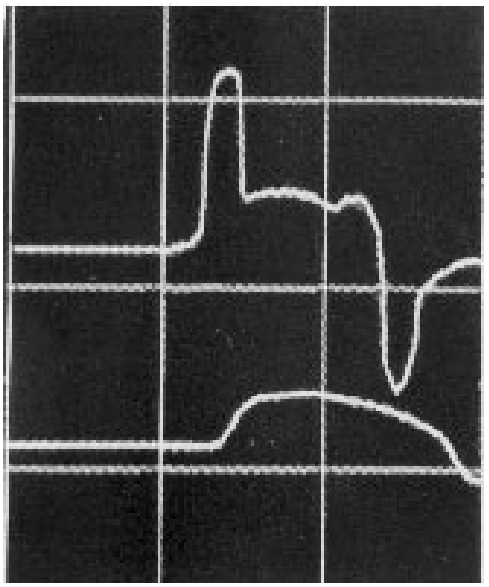

Fig. 5. Typical digital oscilloscope signal of A356·0 aluminum alloy under dynamic torsional loading (1 ms/div for time scale).

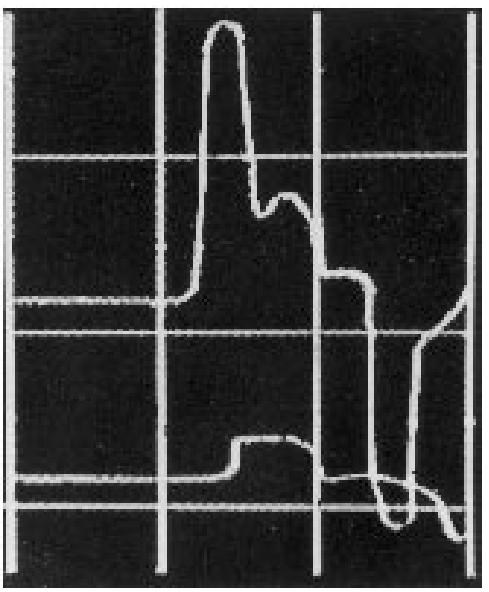

Fig. 6. Typical digital oscilloscope signal of C/A356·0 composite under dynamic torsional loading (1 ms/div for time scale).

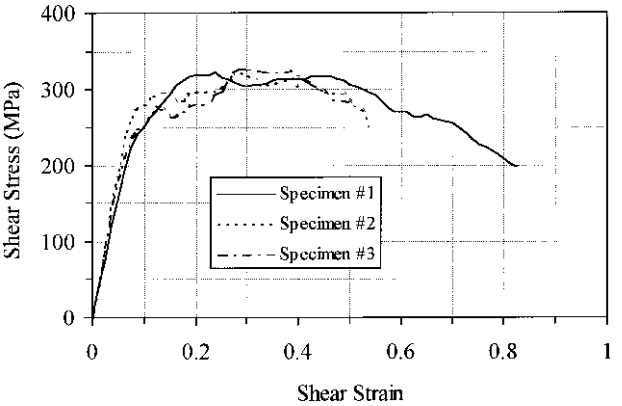

Fig. 7. Dynamic shear stress/strain relationship for A356·0 aluminum alloy.

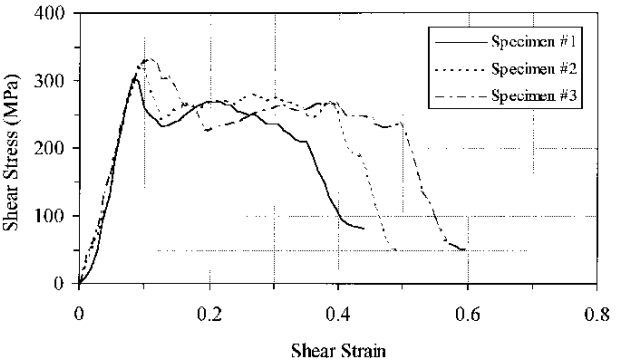

Fig. 8. Dynamic shear stress/strain relationship for C/A356·0 composite.

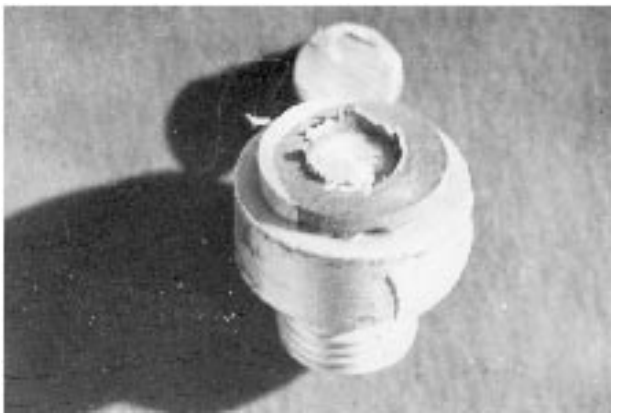

Fig. 9. Typical failure mode of C/A356·0 composite under dynamic torsional loading.

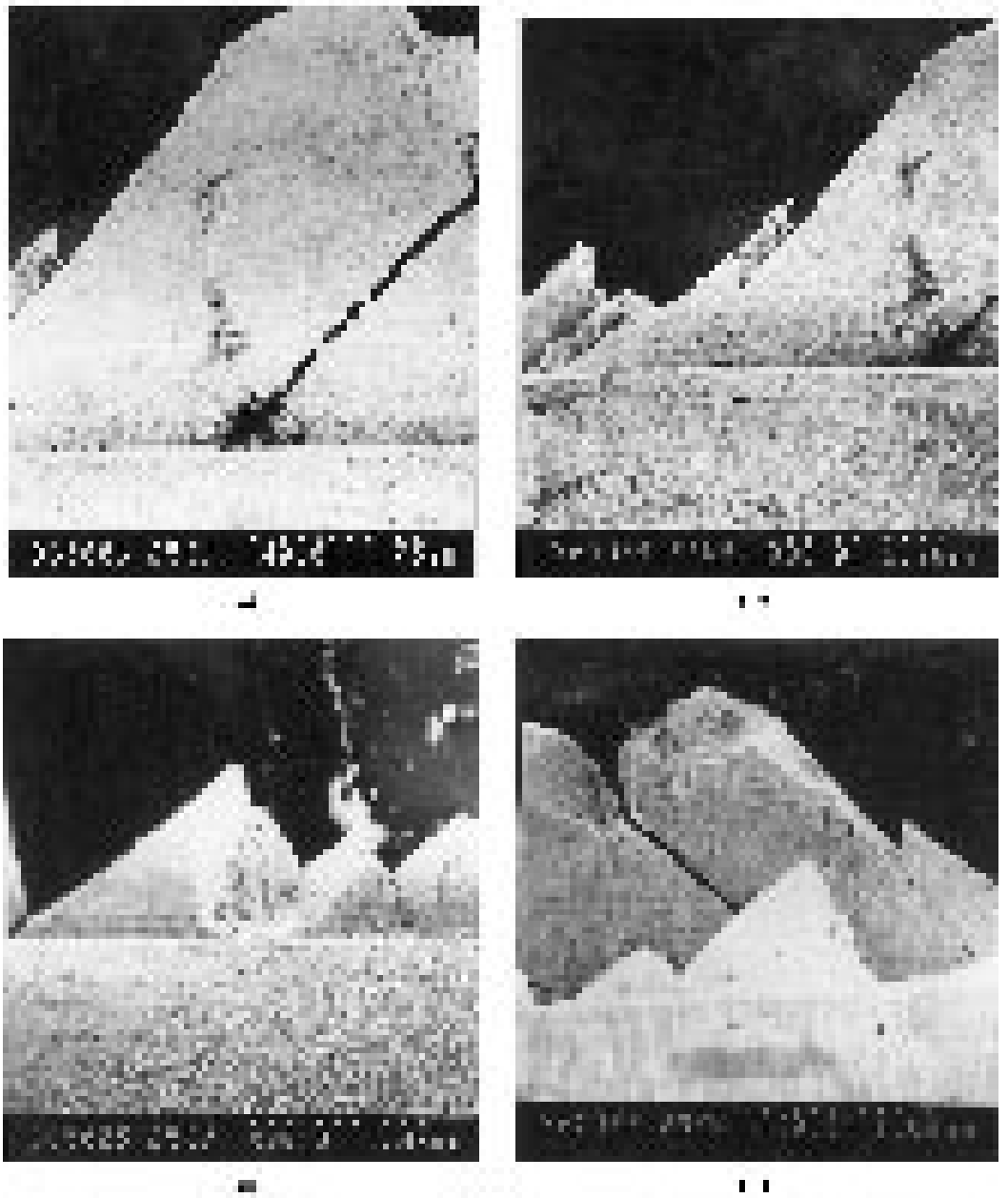

Fig. 10. Micrographs showing the multi-scale zigzag feature at the fracture surface (side view).

pure matrix alloy. Furthermore, it is observed that the shear failure in the composite consists of various stages (see Fig. 8). When the shear strain reaches about 0·1, the load-bearing capacity of the composite falls from the maximum (~330 MPa) to about 260 MPa. Subsequently the composite maintains this stress until the catastrophic failure occurs. It is obvious that this complicated failure process is due to the interaction between the fibers and the matrix in the composite. A typical failure mode of the C/A356·0 composite specimen under dynamic torsional loading is shown in Fig. 9. Moreover, the micrographs by scanning electronic microscopy (SEM) are given in Figs 10 and 11 to present a multi-scale zigzag feature at the fracture surface. This may be due to the tensile failure at 45° to the torsional axis direction. But the failure surface of the matrix does not show such pattern. Therefore, this is a unique feature of shear failure in the unidirectional C/A356·0 composite.

The multi-stage failure process and the multi-scale zigzag fracture surface of the unidirectional C/A356·0 composite imply a complicated shear failure mechanism. It is well known that the macroscopic failure of the materials usually results from the evolution of the nucleation, extension, and coalescence of micro-damage. Each of these micro-mechanical processes is determined by its corresponding stress state. Therefore, in order to understand the shear failure mechanism of the MMCs, a micro-mechanical approach must be adopted to analyze the stress field and the damage evolution at various scales.

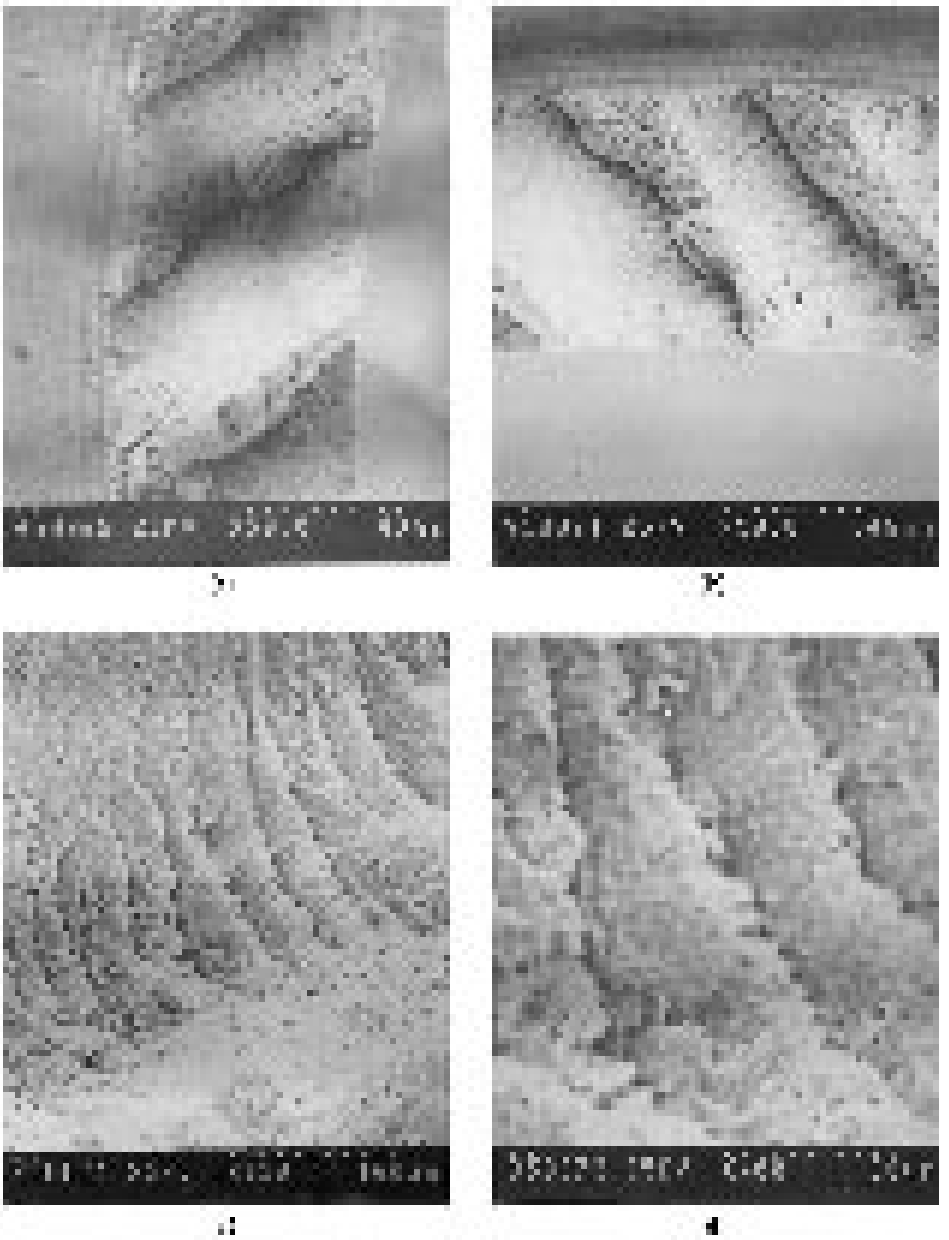

Fig. 11. Micrographs showing the multi-scale zigzag feature at the fracture surface (top view).

4 CONCLUSIONS

In the present study, the dynamic shear strength of both unidirectional C/A356-0 composite and A356-0 aluminum alloy were measured with a split Hopkinson torsional bar apparatus. The results showed that the shear strength of the composite is almost the same as that of the matrix material. This implies that the current carbon fiber orientation which aligns with the torsional loading axis does not improve the shear strength of the matrix effectively. A multi-stage shear failure process and a multi-scale zigzag feature at the fracture surface were identified for the C/A356-0 specimens. This reveals that there is a complicated shear failure mechanism in the unidirectional carbon/aluminum composite under dynamic torsional loading.

ACKNOWLEDGEMENTS

Material preparation by Professor P. X. Qi, S. R. Feng, Y. Z. Wang, L. P. Zhang, and assistance in dynamic testing from Professor L. T. Shen are highly acknowledged.

REFERENCES

1. Parry, T. and Harding, J., The failure of glass-reinforced composites under dynamic torsional loading. In *Plastic Behaviour of Anisotropic Solids*, ed. J. P. Boehler. CNRS, Paris, 1988, pp. 271–288.
2. Chiem, C. Y. and Liu, Z. G., High strain rate behaviour of carbon fiber composites. *Mechanical Behaviour of Composites and Laminates, Proc. European Mechanics Colloquium 214*, ed. W. A. Green and M. Micunovic, Kupari, Yugoslavia, 1986, pp. 45–53.

3. Leber, H. and Lifshitz, J. M., Interlaminar shear behavior of plain-wave GRP at static and high rates of strain. *Compos. Sci. Technol.*, 1996, **56**, 391–405.
4. Werner, S. M. and Dharan, C. K., The dynamic response of graphite fiber-epoxy at high shear strain rates. *J. Compos. Mater.*, 1986, **20**, 365–374.
5. Bouette, B., Cazeneuve, C. and Oytana, C., Effect of strain rate on interlaminar shear properties of carbon-epoxy composites. *Compos. Sci. Technol.*, 1992, **45**, 313–221.
6. Harding, J. and Li, Y. L., Determination of interlaminar shear strength for glass/epoxy and carbon/epoxy laminates at impact rates of strain. *Compos. Sci. Technol.*, 1992, **45**, 161–171.
7. Dond, L. and Harding, J., A single-lap shear specimen for determining the effect of strain rate on the interlaminar shear strength of carbon fiber-reinforced laminates. *Composites*, 1994, **25**, 129–138.
8. Bai, Y. L. and Dodd, B., *Adiabatic Shear Localization*. Pergamon Press, New York, 1992.